STEM CELLS AND DEVELOPMENT
Volume 24, Number 9, 2015

DOI: 10.1089/scd.2014.0321

Antiphotoaging Effect of Conditioned Medium of Dedifferentiated Adipocytes on Skin In Vivo and In Vitro: A Mechanistic Study

Yang Xu,[1] Jia-an Zhang,[1] Yan Xu,[2] Shi-lei Guo,[2] Shen Wang,[1] Di Wu,[1] Ying Wang,[2] Dan Luo,[1] and Bing-rong Zhou[1]

Photoaging of skin occurs partially due to decreased synthesis and increased degradation of dermal collagen. Antiphotoaging therapy aims to counteract these effects. This study aimed to investigate whether secretory factors from dedifferentiated adipocytes (DAs) could alleviate photoaging in human dermal fibroblasts (HDFs) and in mice and to clarify the underlying mechanism. DAs were acquired and verified based on cellular biomarkers and multilineage differentiation potential. The concentrations of several cytokines in conditioned medium from DAs (DA-CM) were determined. In vivo pathological changes, collagen types I and III, and matrix metalloproteinase (MMP)-1 and -3 were evaluated following the injection of 10-fold concentrated DA-CM into photoaged mice. In vitro, the effect of DA-CM on stress-induced premature senescence in HDFs was investigated by 5-ethynyl-2′-deoxyuridine (EdU) staining and β-galactosidase staining. The influence of DA-CM and transforming growth factor-β_1 (TGF-β_1) on the secretion of collagen types I and III, MMP-1, and MMP-3 in HDFs was evaluated by ELISA. In vivo, we found that subcutaneously injected 10-fold concentrated DA-CM increased the expression of collagen types I and III. In vitro, DA-CM clearly mitigated the decreased cell proliferation and delayed the senescence status in HDFs induced by ultraviolet B (UVB). HDFs treated with DA-CM exhibited higher collagen types I and III secretion and significantly lower MMP-1 and MMP-3 secretion. The TGF-β_1-neutralizing antibody could partially reduce the recovery effect. Our results suggest that DAs may be useful for aging skin and their effects are mainly due to secreted factors, especially TGF-β_1, which stimulate collagen synthesis and alleviate collagen degradation in HDFs.

Introduction

Aging of human skin includes intrinsic aging and photoaging. Disorganization, fragmentation, and dispersion of collagen bundles are prominent features of photoaged human skin [1]. Skin fibroblasts synthesize collagen and generate matrix metalloproteinases (MMPs). MMPs can specifically degrade almost all of the extracellular matrix (ECM) components and play an important role in skin photoaging.

Adipose-derived stem cells (ADSCs), which can be obtained from adipose tissue, are reported to exhibit potential advantages in cell therapy for photoaging and wound healing [2–5]. It has been shown that ADSCs can differentiate along multiple lineages, including those of adipocytes, osteoblasts, chondrocytes, myocytes, neuronal cells, and endothelial cells [6,7]. Some studies have shown that ADSCs contribute to skin regeneration through secretion of growth factors [2–5].

However, the stromal cell fraction extracted from adipose tissue is a mixture of fibroblasts, preadipocytes, endothelial cells, and other types of cells [8], and also isolation of ADSCs requires a large volume of adipose tissue. Therefore, other somatic stem cells, if they can be more easily isolated and expanded with high purity, appear more promising.

It has been shown that mature adipocytes can revert to a more primitive phenotype and gain cell proliferative ability when subjected to an in vitro dedifferentiation strategy; these cells are named Das [9]. The surface immunophenotype of dedifferentiated adipocytes (DAs) closely resembles that of bone marrow mesenchymal stem cells and ADSCs. In vitro differentiation analysis revealed that DAs have the capacity to differentiate into adipocytes, chondrocytes, and osteoblasts under appropriate cell culture conditions similar to ADSCs [10]. These indicate that DAs represent a type of multipotent progenitor cell. DAs are obtained from pure mature adipocytes; therefore, they are a more homogeneous population than ADSCs. In addition, it has been shown that DAs can be obtained and expanded from small amounts ($\sim$1 g) of

[1]Department of Dermatology, The First Affiliated Hospital of Nanjing Medical University, Nanjing, China.
[2]Nanjing Regenerative Medicine Engineering and Technology Research Center, Nanjing, China.

adipose tissue [10]. The accessibility and ease of culture of DAs support their potential application in cell-based therapies.

DAs have been shown to contribute to different kinds of tissue repair, including myocardial infarction, bladder injury, and spinal cord injury (SCI)-induced motor dysfunction in model mice [11–13]. However, there is still no report on the antiaging effects of DAs. Therefore, we carried out this study to evaluate the effects of DAs and conditioned medium from DAs (DA-CM) on ultraviolet B (UVB) stress-induced premature senescence (SIPS) in human dermal fibroblasts (HDFs) and photoaged mouse skin. The underlying mechanism was explored.

Materials and Methods

Ethics statement

This study was approved by the ethics committee of the First Affiliated Hospital of Nanjing Medical University and carried out in accordance with the Declaration of Helsinki (2000). All the people were informed of the purpose and procedure of this study and they agreed to offer their tissue specimens. Written consent was obtained from the participants involved in this study. The animal experiments were approved by the Animal Care and Use Committee in Nanjing Medical University.

Isolation and culture of DAs

Isolation of mature adipocytes from human fat tissue was performed using a modification of the method described previously by Sugihara et al. [14]. Adipose tissue was taken by liposuction from a healthy adult. The adipose tissue was promptly washed with sterile phosphate-buffered saline (PBS) and visible blood vessels were removed. The sample was minced into smaller pieces and treated with 0.2% type I collagenase (GIBCO, Invitrogen) at 37°C for 35–40 min on a constant shaker at 200 rpm. The collagenase activity was terminated by addition of an equal volume of complete medium consisting of low glucose Dulbecco's modified Eagle's medium (DMEM; GIBCO), 10% fetal bovine serum (FBS; GIBCO), and 1% penicillin–streptomycin solution (Beyotime Institute of Biotechnology), and the cell suspension was centrifuged for 3 min at 1,000 rpm. The floating top layer containing unilocular adipocytes was harvested and seeded at a density of $0.5–1 \times 10^6$ cells per 25-cm^2 flask. The flasks were fully filled with complete culture medium, which ensured that the floating cells were able to attach to the inner top surface of the flask. The cells were incubated at 37°C in 5% CO_2; this is termed ceiling culture. After 48 h, the flasks were inverted back. The medium was changed every 3 days until the cells reached confluence. The cells were used for further experiments between passages 3 and 5.

Adipogenic, osteogenic, and chondrogenic differentiation assays of DAs

We performed three different in vitro experiments to evaluate the multilineage differentiation potential of DAs, as instructed by Matsumoto [10]. After 2 weeks, cells were stained by Oil Red O, Alizarin red, and Alcian blue to visualize intracellular lipid droplets, calcium accumulation, and the chondrocyte matrix, respectively.

Flow cytometry analysis of biomarkers of DAs

DA samples were characterized by flow cytometry after the third passage. Cells were digested with pancreatin and stained with FITC-, PE-, or PerCP-conjugated antibodies against CD34, CD71, CD90, and CD29, respectively. Cells were analyzed by a FACSCalibur flow cytometer (BD Biosciences). Positive cells were counted and their signals compared with that from the corresponding immunoglobulin isotypes.

Detection of secretory factors in DA-CM by ELISA

DAs were cultured for 48 h and the conditioned medium was collected for measurement of growth factors. ELISA kits were used as instructed (R&D Biosystems) to detect the concentrations of platelet-derived growth factor-BB (PDGF-BB), basic fibroblast growth factor (bFGF), vascular endothelial growth factor (VEGF), keratinocyte growth factor (KGF), transforming growth factor-β_1 (TGF-β_1), and hepatocyte growth factor (HGF).

Collection and concentrate of conditioned medium from cultured DAs

DAs, between passages 3 to 5, were cultured in 6-cm plates. The conditioned medium was collected when cells reached to, or were greater than, 80% confluence. The medium was first centrifuged at 10,000 *g* for 15 min (4°C) and filtered with a 0.22-μm filter, and then concentrated to 10-fold in DMEM by ultrafiltration using Centriprep® 3K filter units (Merck Millipore Ltd.) at 3,000 *g* for 50 min once and for 10 min twice at 4°C, as instructed. DMEM also underwent the same procedure to get desalinated and concentrated as the control for further experiment in vivo. The supernatants were stored at −80°C within 1 week for further use.

Tracking of DAs in nude mice skin

Eight immunodeficient nude mice (female, 8 weeks old) and all other mice used in this study were purchased from the Animal Center of Nanjing University and kept under controlled humidity (40%) and temperature (22°C ± 2°C). DAs were labeled by the PKH26 Red Fluorescent Cell Linker Kit (Sigma-Aldrich, Inc.) in accordance with the instructions. The injectable poloxamer-octapeptide hybrid hydrogel was prepared as we described before [15,16]. One milliliter of hydrogel containing 10^5 DAs labeled by PKH26 was subcutaneously injected at two places, each on one side of dorsal skin. Punch biopsies were conducted from the injection sites for immunofluorescence examination after 4 and 8 weeks, respectively. Pictures were taken under ×200 magnification under an immunofluorescent microscope.

Histopathological analysis of changes in nude mice skin caused by DAs

One milliliter of hydrogel with DAs (10^5 cells/1 mL) was subcutaneously injected with a 26-gauge needle at two places on one side of dorsal skin of every eight immunodeficient nude mice (female, 8 weeks old). For the control side, the same volume of hydrogel without DAs was subcutaneously injected at the similar places. Four and 8 weeks

after injection, punch biopsies were taken, formalin fixed, paraffin embedded, sliced, and stained with hematoxylin and eosin (H&E) and Masson trichrome to evaluate morphological changes. The pictures were taken under ×200 magnification. The thicknesses of the dermis and epidermis by H&E staining were measured by ImageJ (http://rsbweb.nih.gov/ij/) by a blinded observer, and the relative thickness of the dermis (the ratio of thickness of dermis to that of dermis plus epidermis) was calculated. The Masson staining positive areas were analyzed by ImageJ, also by a blinded observer, and the average percentage of the stained area was calculated.

Establishment of the UVB-induced photoaged mouse model and treatment with DA-CM

Eight BALB/c mice (female, 8 weeks old) were used. UVB-induced photoaging mice were obtained as previously reported [17]. Briefly, the mice were shaved and irradiated by UVB (311 ± 10 nm) with a solar simulator (Sigma) five times a week for 8 weeks. The irradiation intensity represented as the minimal erythema dose (MED) was set at one MED during the first 2 weeks (60 mJ/cm^2), elevated to two MED (120 mJ/cm^2) in the 3rd week, to three MED (180 mJ/cm^2) in the 4th week, and to four MED (240 mJ/cm^2) during the last 4 weeks of the experiment. The total irradiated UVB dosage was ∼115 MED (6.9 J/cm^2).

To study the effect of DA-CM on photoaged mouse skin, 200 μL of 10-fold concentrated DA-CM was subcutaneously injected into two places in the skin of eight photoaged mice, with 200 μL of 10-fold concentrated DMEM injected into the other side as control. The injections were conducted once a week for a total of three times. After 4 and 8 weeks, skin samples were taken for further study.

Histopathological analysis of changes in photoaged mice skin caused by DA-CM

Four and 8 weeks after the first injection, punch biopsy specimens were taken, and histopathological changes were observed by H&E and Masson trichrome staining by a blinded observer. The thicknesses of the dermis and epidermis and the Masson positive-stained area were measured by ImageJ. The relative thickness of the dermis and average percentage of the stained area by Masson trichrome were calculated.

Immunohistological analysis of collagen types I and III, MMP-1, and MMP-3

The primary antibodies were used against collagen type I (Santa Cruz Biotechnology) and collagen type III (Boster), MMP-1(Boster), and MMP-3 (Boster). Formalin-fixed paraffin-embedded sections (6 μm) were deparaffinized, rehydrated, and then treated with 0.01 M sodium citrate buffer. The sections were incubated with primary antibodies against collagen types I (200 μg/mL diluted by 1:150) and III (200 μg/mL diluted by 1:150), MMP-1 (200 μg/mL diluted by 1:50), and MMP-3 (200 μg/mL diluted by 1:50) overnight at 4°C. After the sections were washed in PBS, bovine serum-free DMEM was added, and the sections were further incubated in the secondary antibody IgG for 20 min and then reacted with the streptavidin-biotin-peroxidase complex (SABC) and 3,3′-diaminobenzidine (DAB) substrate solution. The results were visualized under the light microscope at 200× magnification by a blinded observer. Controls without primary antibodies showed no immunolabeling. Light brown to dark brown staining indicated a positive result. The stained areas were analyzed by ImageJ. The average percentage of stained area was calculated.

SIPS in HDFs induced by UVB

HDFs derived from the foreskin of a 20-year-old donor with informed consent were isolated and cultured in DMEM supplemented with 2 mM glutamine and 10% FBS at 37°C in 5% CO_2. At 70%–80% confluence, the cells were subcultured and divided into the following subgroups: HDFs (HDFs cultured in serum-free DMEM), SIPS-HDFs (HDFs cultured in serum-free DMEM and exposed to UVB irradiation), DA-CM-treated HDFs (HDFs cultured in DA-CM), and DA-CM-treated SIPS-HDFs (HDFs cultured in DA-CM and exposed to UVB irradiation). SIPS was established in HDFs by repeated UVB irradiation, as previously reported [18,19]. Briefly, the cells were ultraviolet (UV) irradiated in a thin layer of PBS in a plastic dish without lids using a solar simulator (Sigma). The intensity of the radiation from the UVB source was measured before each experiment using a UVR radiometer with a UVB sensor (Bioblock Scientific). The irradiation distance between the cultured cells and the UV source was 15 cm and the irradiation dosage per day was 10 mJ/cm^2 controlled by a radiometer. Radiation stress was performed once a day for 5 days. For the sham-irradiated groups, HDFs were handled identically, except that they were shielded with aluminum foil during the irradiation.

Proliferation assay of HDFs with the presence of TGF-β_1-neutralizing antibody

The TGF-β_1-neutralizing antibody (R&D Biosystems) was added into the supernatants of HDFs at a concentration of 0.2 μg/mL. After 24 h, cell proliferation was assayed using a CCK-8 Kit as described before.

Measurement of cell proliferation and cellular senescence of HDFs

For DA-CM-treated groups, sham or UV-irradiated HDFs were cultured in media containing 2 mL of 10-fold concentrated DA-CM following every irradiation in six-well plates. For the control group, sham or UV-irradiated HDFs were cultured in serum-free DMEM. After 2 days of UVB irradiation, four groups, including the HDF group, SIPS-HDF group, HDF + DA-CM group, and SIPS-HDF + DA-CM group, were evaluated for cell growth by the CCK-8 method and 5-ethynyl-2′-deoxyuridine (EdU) fluorescence staining and also for cellular senescence by β-galactosidase staining.

For the process of using a CCK-8 Kit (Beyotime), 100 μL of cells (2×10^3 cells/well) was transferred into 96-well plates after digestion with trypsin, and other parallel wells were used for each treatment. After attachment, the cells were subjected to the different treatments and then cultured for 24 h in a 5% CO_2 incubator at 37°C. Subsequently, 10 μL CCK-8 was added to each well, and the cells were cultured for another 3 h. Cell density was determined by

measuring the absorbance at 450 nm using a Varioskan Flash (Thermo Scientific).

To determine EdU uptake, we measured the incorporation of EdU into the DNA strand using an EdU assay kit (Ribobio) according to the manufacturer's instructions. Briefly, four groups of cells were exposed to 50 μM of EdU for 2 h at 37°C, and cells were fixed by 4% formaldehyde for 15 min at room temperature and treated with 0.5% Triton X-100 for 20 min at room temperature for permeabilization. After washing thrice with PBS, each well was treated with 100 μL of 1× Apollo® reaction cocktail for 30 min. Subsequently, the Hoechst 33342 solution with a final concentration of 10 μg/mL was used for staining nuclei. The ratio of positive EdU staining cells was calculated.

We confirmed the photoaging of HDFs based on cell flattening and positive β-galactosidase staining using the SA-β-gal staining kit (Beyotime). The percentages of positively stained cells in every field were calculated thrice for every group by a blinded observer. Four groups, including the HDF group, SIPS-HDF group, HDF + DA-CM group, and SIPS-HDF + DA-CM group, were evaluated for cellular senescence of fibroblasts.

Furthermore, the effects of TGF-β_1 in DA-CM on cellular premature senescence of HDFs were studied. Three groups, including the SIPS-HDF group, SIPS-HDF + DA-CM group, and SIPS-HDF + DA-CM + anti-TGF-β_1 group (0.2 μg/mL TGF-β_1-neutralizing antibody were added), were also stained by SA-β-gal staining. The percentages of positively stained cells were calculated thrice for every group by a blinded observer.

Measurement of collagen types I and III, MMP-1, and MMP-3 proteins in HDFs and UV-irradiated HDFs influenced by DA-CM using ELISA

HDFs were irradiated with UVB as described above with a single dosage of 30 mJ/cm^2. For the DA-CM-treated group, sham or UV-irradiated HDFs were cultured in media containing 2 mL of 10-fold concentrated DA-CM. The supernatants from every group were taken for ELISA determination of the concentrations of collagen types I and III (Mybiosource), MMP-1 (R&D Biosystems), and MMP-3 (R&D Biosystems) after 6, 12, 24, and 48 h of UVB irradiation.

ELISA measurement of influence of TGF-β_1 on the effect of DA-CM on UV-irradiated HDFs

HDFs were irradiated with UVB as described above with a single dosage of 30 mJ/cm^2. Subsequently, the same volumes of bovine serum-free DMEM, 10-fold concentrated DA-CM, and 10-fold concentrated DA-CM with 0.2 μg/mL TGF-β_1-neutralizing antibody were added individually to three separate groups as follows: UV-HDF group, DA-CM-treated UV-HDF group, and DA-CM + anti-TGF-β_1-treated UV-HDF group. The concentrations of collagen types I and III, MMP-1, and MMP-3 secreted by HDFs were detected using an ELISA kit according to the manufacturer's instructions as described above for these three groups after culture for 24 and 48 h.

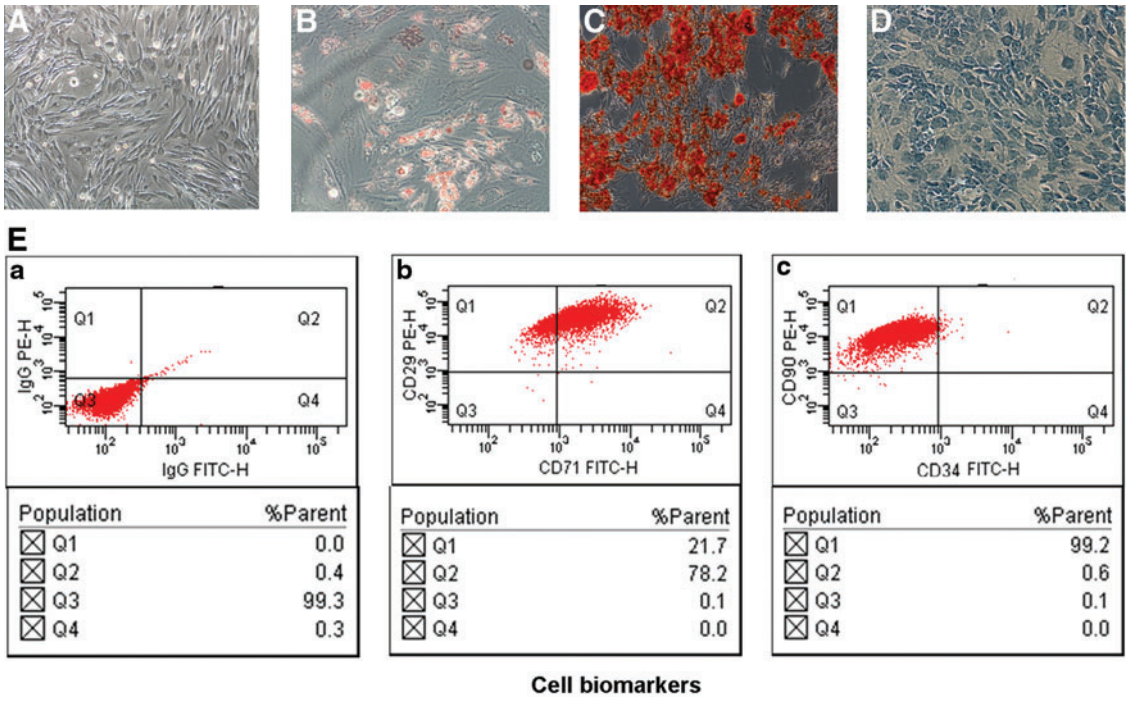

FIG. 1. DAs exhibit multipotent differentiation potential and stem cell-like characteristics in vitro. **(A)** Bright-field view of fibroblast-like morphologic appearance in cultured DAs. **(B–D)** DAs were cultured in specialized medium for 2 weeks as described in the Materials and Methods section. The cells were analyzed for **(B)** adipogenic (Oil Red O), **(C)** osteoblasts (Alizarin red S), and **(D)** chondrogenic (Alcian blue) capacity. **(E)** Flow cytometry analysis of DAs for the expression of CD29, CD71 **(b)**, CD90, and CD34 **(c)** on the surface of DAs. Mouse IgG **(a)** is a negative control for the analysis. DAs, dedifferentiated adipocytes. Color images available online at www.liebertpub.com/scd

Table 1. Concentrations of Secreted Growth Factors in the Conditioned Medium of Dedifferentiated Adipocytes (Per 10^7 Cells)

Cytokines	*Concentrations (pg/mL)*
PDGF-BB	16.04 ± 2.57
bFGF	25.34 ± 5.41
KGF	13.27 ± 2.76
TGF-β_1	24.83 ± 9.42
HGF	85.57 ± 25.33
VEGF	176.42 ± 23.67

bFGF, basic fibroblast growth factor; HGF, hepatocyte growth factor; KGF, keratinocyte growth factor; PDGF-BB, platelet-derived growth factor-BB; TGF-β_1, transforming growth factor-β_1; VEGF, vascular endothelial growth factor.

Statistical analysis

All experiments in vitro were performed at least thrice in triplicate and data were statistically analyzed using SPSS 11.0 Software. The values in the figures are expressed as mean ± SD. Paired *t*-test was used for statistical analysis of the results, with $P < 0.05$ considered statistically significant.

Results

DAs exhibit multipotent differentiation potential and stem cell-like characteristics

The DAs isolated and cultured from adult human fat tissue expanded easily in vitro and exhibited fibroblast-like morphology (Fig. 1A). The cells also exhibited multipotent differentiation potential when cultured in the specialized medium for 2 weeks as described in the Materials and Methods section. The characteristic staining of Oil Red O, Alizarin red S, and Alcian blue illustrated that DAs, like reported ADSCs, are able to differentiate into adipocytes, osteoblasts, and chondrocytes (Fig. 1B–D).In addition, the DAs also exhibit characteristic expression of stem cell-related surface markers measured by flow cytometry, which includes expression of CD29, CD71, and CD90, but not CD34 (Fig. 1E).

It has been reported that ADSCs are able to produce a variety of growth factors; we therefore determined whether DAs had similar capability. As shown in Table 1, the growth factors, including PGDF-BB, bFGF, KGF, TGF-β_1, HGF, and VEGF, were easily detected from the conditioned medium collected from DA cultures.

These lines of evidence provide the solid evidence that the spindle-like cells we obtained are DAs, which possess the stem cell-like feature of differentiation and produce a variety of growth factors like ADSCs.

DAs colonize and proliferate in adipose tissue and increase the thickness of the dermis and density of collagen in nude mice skin

To track the localization of injected DAs in the mouse skin, DAs were labeled with a red fluorescent dye PKH26 before injection. Under a fluorescence microscope, intensive red fluorescence was only observed in the fat layer where the injection were performed after 4 and 8 weeks, and no fluorescence was found in the epidermis and dermis, indicating that the subcutaneously injected DAs colonized and proliferated in the fat layer at least up to 8 weeks (Fig. 2).

Four weeks and 8 weeks after subcutaneous injection of DAs, the pathological finding showed DAs could significantly improve the content of collagen in the dermis. On H&E staining, the relative thickness of the dermis (control: 0.83 ± 0.03, DA: 0.92 ± 0.02, $*P < 0.05$) and density of collagens increased gradually at the 4th week, showing the largest amounts at the end (the 8th week: control: 0.84 ± 0.01, DA: 0.95 ± 0.01, $*P < 0.05$) of the observation (Fig. 3A, C). At the same time, the collagen fibers were arranged in a better order and in parallel to the epidermal surface, and also appearing as the increase of the density of dermal collagen (4 weeks: control: 36.61% ± 1.79%, DA: 62.21% ± 2.82%, $*P < 0.05$; 8 weeks: control: 42.82% ± 4.54%, DA: 84.07% ± 3.49%, $*P < 0.05$) with orderly arrangement in slices with Masson trichrome staining (Fig. 3B, D), which was also confirmed by V.G staining (Supplementary Fig. S1; Supplementary Data are available online at www.liebertpub.com/scd).

DA-CM mitigates the reduction of collagen types I and III induced by UVB irradiation

UV irradiation-induced skin aging has been extensively studied in vivo and in vitro. To determine whether DA-CM is able to alter UV effects on skin aging, we first established

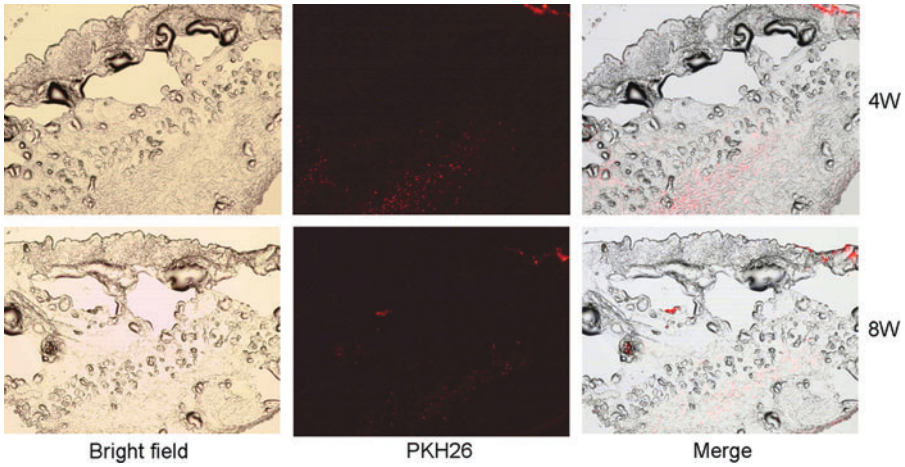

FIG. 2. Tracking PKH26-labeled DAs in nude mice skin. One milliliter of hydrogel containing 10^5 DAs labeled by PKH26 was subcutaneously injected into nude mice. Punch biopsies were taken 4 and 8 weeks post injection, respectively, for immunofluorescence examination. Red fluorescent cells represent cells from injected DAs. Pictures were taken under ×200 magnification under an immunofluorescence microscope. Color images available online at www.liebertpub.com/scd

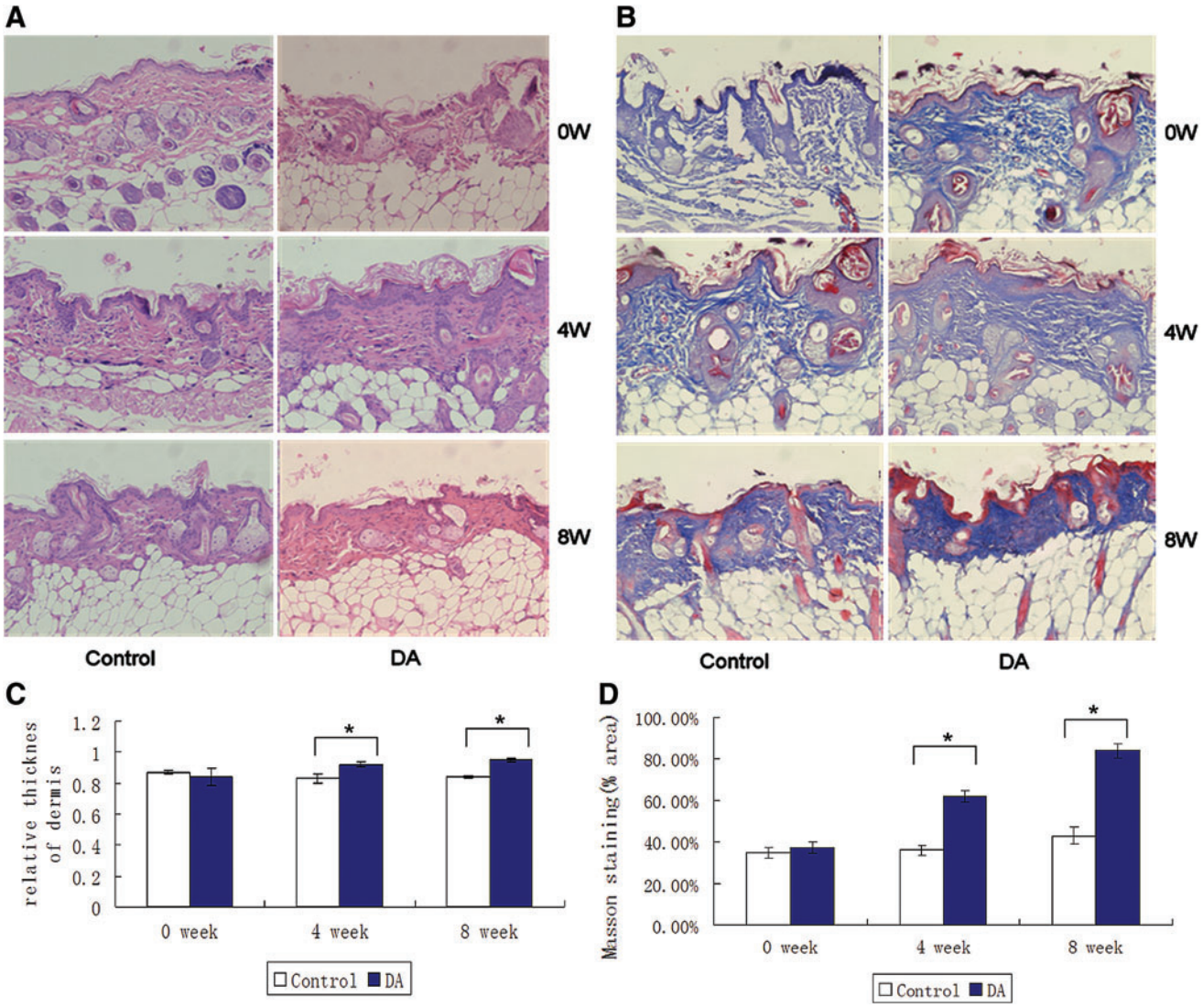

FIG. 3. Subcutaneous injection of DAs increases the thickness of the dermis and improves the density and arrangement of collagen fibers in the dermis of nude mice skin. One milliliter of hydrogel with DAs (10^5/mL) was subcutaneously injected into nude mice skin. Punch biopsies were taken 4 and 8 weeks post injection for staining either with H&E **(A)** or Masson trichrome **(B)**. Collagen fibers were stained *blue* and background *red*. The pictures were taken under ×200 magnification. The thicknesses of the dermis and epidermis by H&E staining were measured by ImageJ and the relative thickness of the dermis (the ratio of thickness of dermis to that of dermis plus epidermis) was calculated **(C)**. The Masson staining positive areas were analyzed by ImageJ and the average percentage of stained area was calculated **(D)**. Data are mean ± SD, $n = 8$, $^*P < 0.05$ versus injection of same volume of hydrogel without DAs as a control. H&E, hematoxylin and eosin. Color images available online at www.liebertpub.com/scd

the UVB-induced photoaged mouse model. Histological analysis, based on H&E, exhibited a significant appearance of thicker epidermis and less and loose collagen in the dermis compared with nonUV-irradiated mouse skin (Supplementary Fig. S2). Next, we determined the DA-CM effects on the photoaged mouse model, and a significant increasing of collagen amount and improving organization of collagen fibrils in the dermis were observed at 4 weeks (positive-stained area: control: 19.78% ± 2.01%, DA-CM: 34.31% ± 3.44%, $^*P < 0.05$) and 8 weeks (control: 19.35% ± 2.53%, DA-CM: 49.33% ± 4.78%, $^*P < 0.05$) post DA-CM injection (Fig. 4).

In correspondence with the pathological findings, at weeks 4 and 8, the section from the DA-CM-injected side exhibited deeper brown staining for collagen type I (Fig. 5A, C) and collagen type III proteins (Fig. 5B, D) compared with the control side. The observations were further confirmed by quantitative assessment of the percentage of collagen I expression (in terms of stained area) by ImageJ, which showed that expression of collagen I significantly increased at week 4 (control: 19.01% ± 2.22%, DA-CM: 23.14% ± 2.43%, $^*P < 0.05$) and remained elevated to week 8 (control: 22.02% ± 3.41%, DA-CM: 45.37% ± 3.07%, $^*P < 0.05$) post DA-CM injection. Similar results were observed upon staining for collagen type III at week 4 (control: 23.31% ± 1.34%, DA-CM: 45.93% ± 3.50%, $^*P < 0.05$) and week 8 (control: 23.02% ± 2.42% DA-CM: 56.94% ± 6.63%, $^*P < 0.05$). However, no obvious changes in the expression of MMP-1 (Fig. 6A,

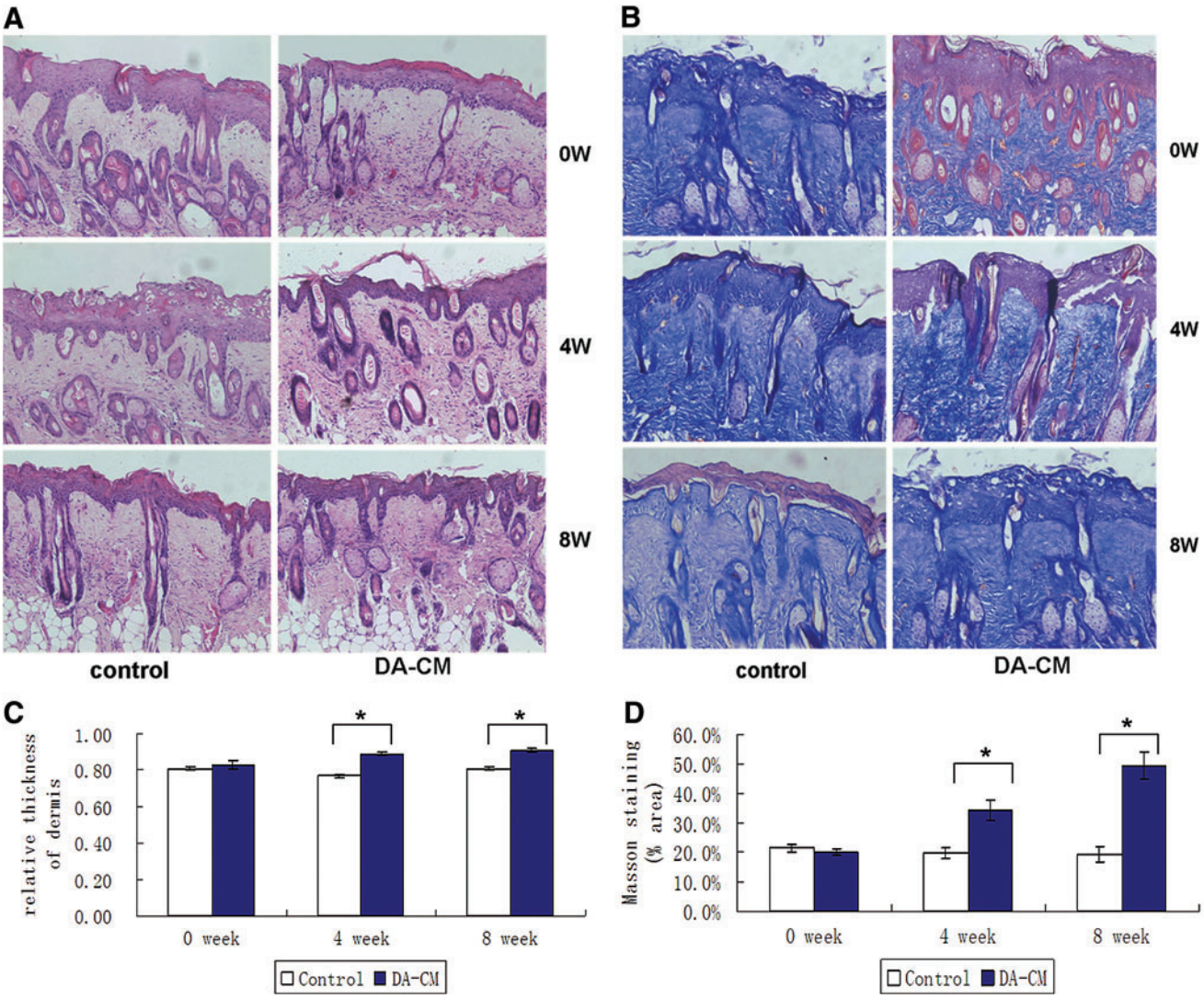

FIG. 4. Subcutaneous injection of DA-CM alleviates the reduction of collagen and improves the arrangement of collagen in the photoaged mouse skin dermis. Two hundred microliters of concentrated DA-CM was subcutaneously injected into the skin of photoaged mice. Skin samples were taken on indicated days and subjected to stain with H&E **(A)** and Masson trichrome **(B)**. Collagen fibers were stained *blue* and background *red*. The pictures were taken under ×200 magnification. The thicknesses of the dermis and epidermis by H&E staining were measured by ImageJ and the relative thickness of the dermis (the ratio of thickness of dermis to that of dermis plus epidermis) was calculated **(C)**. The Masson staining positive areas were analyzed by ImageJ and the average percentage of stained area was calculated **(D)**. Data are mean ± SD, $n = 8$, $^*P < 0.05$ versus injection of same volume of concentrated DMEM as a control. DA-CM, conditioned medium from DA. Color images available online at www.liebertpub.com/scd

C) and MMP-3 (Fig. 6B, D) were observed compared with the control, probably because MMP-1 and MMP-3 were predominantly expressed in the epidermis. Taken together, these results demonstrate that subcutaneously injected DA-CM can mitigate UVB effects on collagen types I and III expression in a time-dependent manner.

DA-CM mitigates UVB-induced changes in cell proliferation and premature senescence in cultured HDFs

It has been known that UVB irradiation inhibits cell growth and leads to cell premature senescence. To investigate the impact of DA-CM on the cell growth after UVB exposure, we performed cell proliferation analysis. As shown in Fig. 7A and B, after UVB irradiation, the percentage of EdU-positive cells increased significantly compared with control cells (HDF: 66.01% ± 5.01%, SIPS-HDF: 10.33% ± 1.23%, $^*P < 0.05$), indicating less cells in the S phase after UVB irradiation. With DA-CM treatment, the decreased proliferation by UVB irradiation was dramatically increased, with increased percentage of EdU-positive cells (SIPS-HDF + DA-CM: 52.07% ± 4.04%, $^*P < 0.05$). The CCK-8 assay confirmed the result that UVB irradiation inhibits cell proliferation and DA-CM could mitigate this effect (Fig. 7C, $^*P < 0.05$).

Next, we determined the impact of DA-CM on cell premature senescence. As Fig. 8 shows, HDFs, experiencing

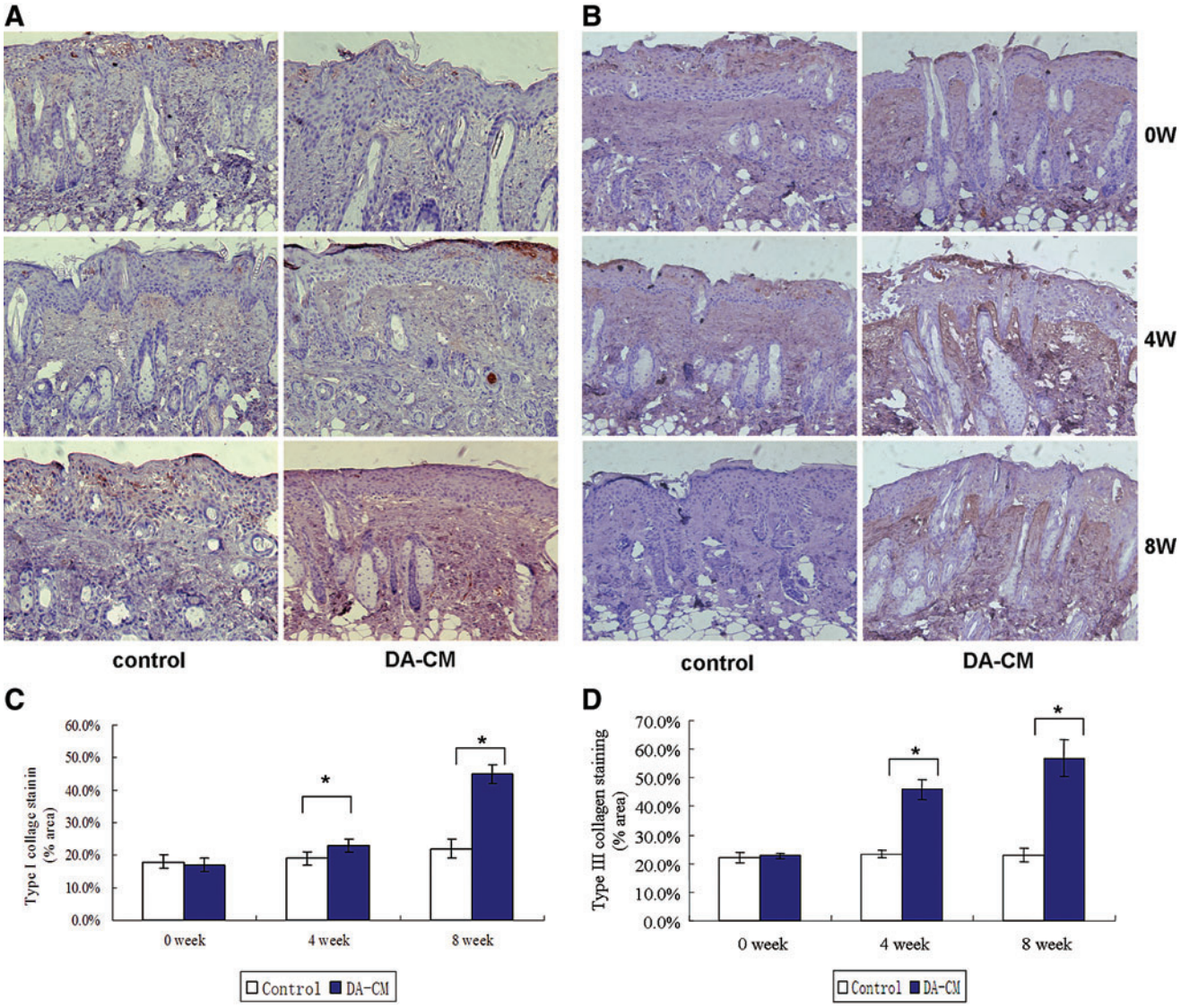

FIG. 5. Subcutaneous injection of concentrated DA-CM increases the collagen types I and III expression in photoaged mouse dermis. Skin punch biopsies were taken at indicated days post injection of concentrated DA-CM in the mouse skin. Immunohistological staining for collagen type I **(A)** and collagen type III **(B)** was measured. The pictures were taken under ×200 magnification. Quantification of the protein levels of collagen type I **(C)** and collagen type III **(D)** was measured by ImageJ. Data are mean ± SD, $n = 8$, $^*P < 0.05$ versus injection of same volume of concentrated DMEM as a control. Color images available online at www.liebertpub.com/scd

UVB irradiation for 5 consecutive days (SIPS-HDF group), exhibited significant changes in appearance from spindle like to large, flat, and irregular in shape (Fig. 8, upper right panel) compared with the HDF group (Fig. 8, upper left panel). Premature senescence staining revealed that while 8.81% of cells in the HDF group presented SA-β-gal staining, 97.12% of cells in the SIPS-HDF group were intensively stained with SA-β-gal. However, on addition of DA-CM to HDFs, we observed that DA-CM alleviated the increased senescent staining by repeated UVB irradiation, and cells with SA-β-gal staining were reduced to 41.43% (Fig. 8, lower right panel).

These data indicate that DA-CM could alleviate the decreased cell proliferation and delay premature senescence occurrence induced by UVB, indicating the antiphoto damage effect.

TGF-β_1 regulates the protection effect of DA-CM on UVB-induced premature senescence in cultured HDFs

We detected TGF-β_1 in DA-CM (Table 1). To confirm the hypothesis that DA-CM prevents UV effects through secretion of TGF-β_1, we added the TGF-β_1-neutralizing antibody (0.2 μg/mL) to HDFs cultured with DA-CM, and cell proliferation assay showed no obvious difference in cell numbers within 48 h post TGF-β_1-neutralizing antibody addition compared with the cells added with control IgG (Fig. 9), indicating that the neutralizing antibody at this concentration does not cause harm to the cell viability. Furthermore, premature senescence staining revealed that while 97.92% of cells in the SIPS-HDF group and 39.72% of cells in

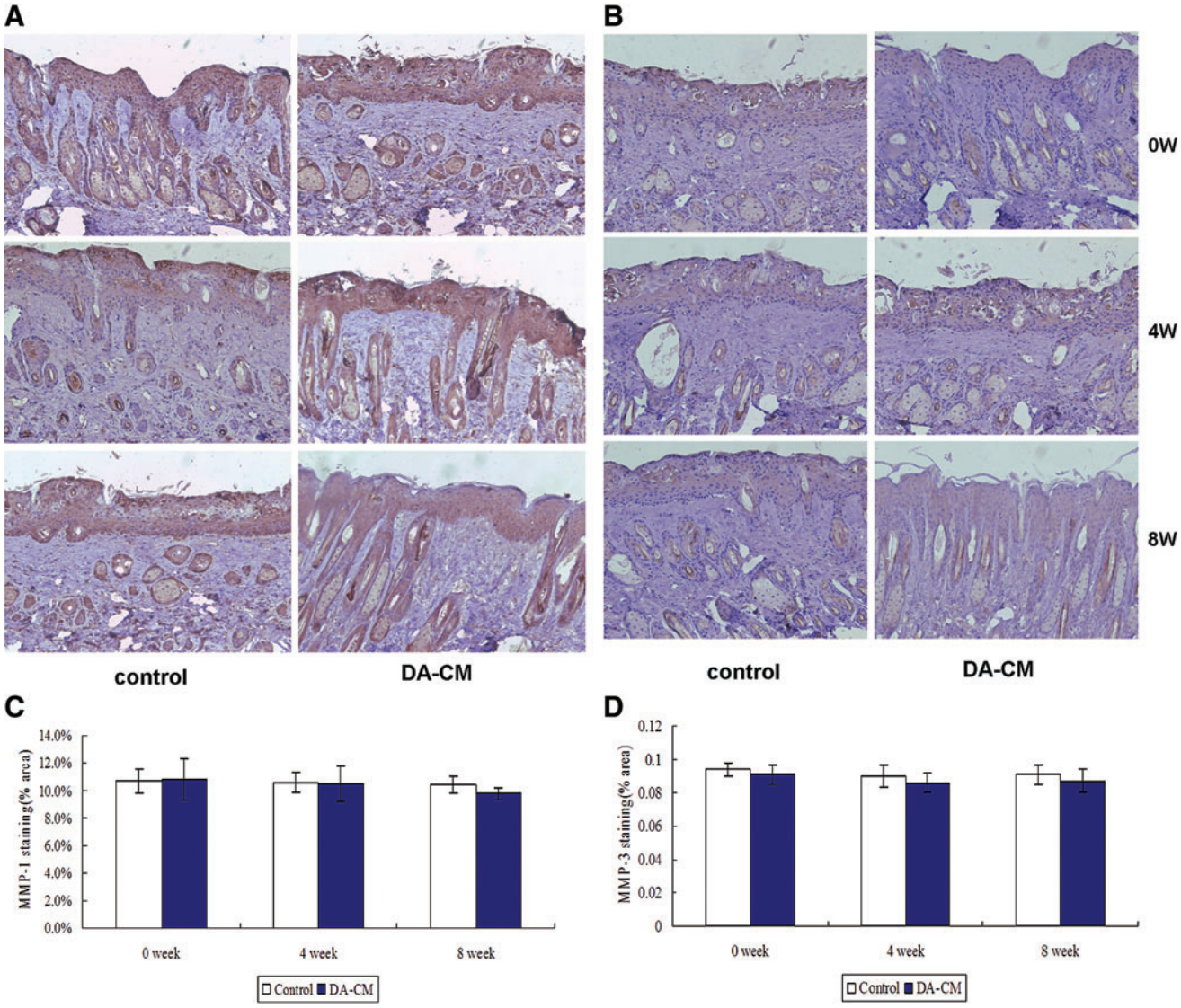

FIG. 6. Subcutaneous injection of concentrated DA-CM does not alter the induction of MMP-1 and MMP-3 in photoaged mouse dermis. Skin punch biopsies were taken at indicated days post injection of concentrated DA-CM in the mouse skin. Immunohistological staining for MMP-1 **(A)** and MMP-3 **(B)** was measured. The pictures were taken under ×200 magnification. Quantification of the protein levels of MMP-1 **(C)** and MMP-3 **(D)** was measured by ImageJ. Data are mean ± SD, $n = 8$. MMP, matrix metalloproteinase. Color images available online at www.liebertpub.com/scd

SIPS-HDF + DA-CM were intensively stained with SA-β-gal, addition of anti-TGF-β_1-neutralizing antibody mitigated the effects of DA-CM on SIPS-HDFs with the percentage of positive staining cells increased to 47.84% (Fig. 10), indicating that TGF-β_1 plays an important role in DA-CM during the antipremature senescence process caused by UVB irradiation.

DA-CM prevented UVB effects on the alteration of collagen type I, type III, MMP-1, and MMP-3 proteins in HDFs

Our in vivo study shows that DA-CM mitigated UVB effects on reduction of collagen type I and III proteins (Fig. 11). It would stand to reason whether DA-CM was able to overcome UVB effects in cultured HDFs. We observed that, from 24 to 48 h after UV irradiation, both collagen type I (HDF + UV group, 86.44 ± 2.11 ng/mL at 24 h, 105.34 ± 2.49 ng/mL at 48 h) and type III (HDF + UV group, 1.08 ± 0.04 ng/mL at 24 h, 1.19 ± 0.11 ng/mL at 48 h) were dramatically reduced compared with nonUV-irradiated HDFs (HDF group, collagen type I: 123.09 ± 1.81 ng/mL at 24 h, 137.55 ± 1.97 ng/mL at 48 h; collagen type III: 1.64 ± 0.11 ng/mL at 24 h, 1.88 ± 0.06 ng/mL at 48 h). However, addition of DA-CM to cultured HDFs largely prevented this reduction by UV irradiation (Fig. 11A, B, HDF + UV + DA-CM group, collagen type I: 101.77 ± 1.95 ng/mL at 24 h, 127.05 ± 2.57 ng/mL at 48 h; collagen type III: 1.57 ± 0.10 ng/mL at 24 h, 1.61 ± 0.09 ng/mL at 48 h).Administration of DA-CM also effectively prevented induction of MMP-1 and MMP-3 proteins by UV irradiation (Fig. 11C, D; HDF + UV group vs. HDF + UV + DA-CM group: 11.12 ± 0.19 vs. 5.42 ± 0.12 ng/mL at 24 h and 13.76 ± 0.25 vs. 6.19 ± 0.17 ng/mL at

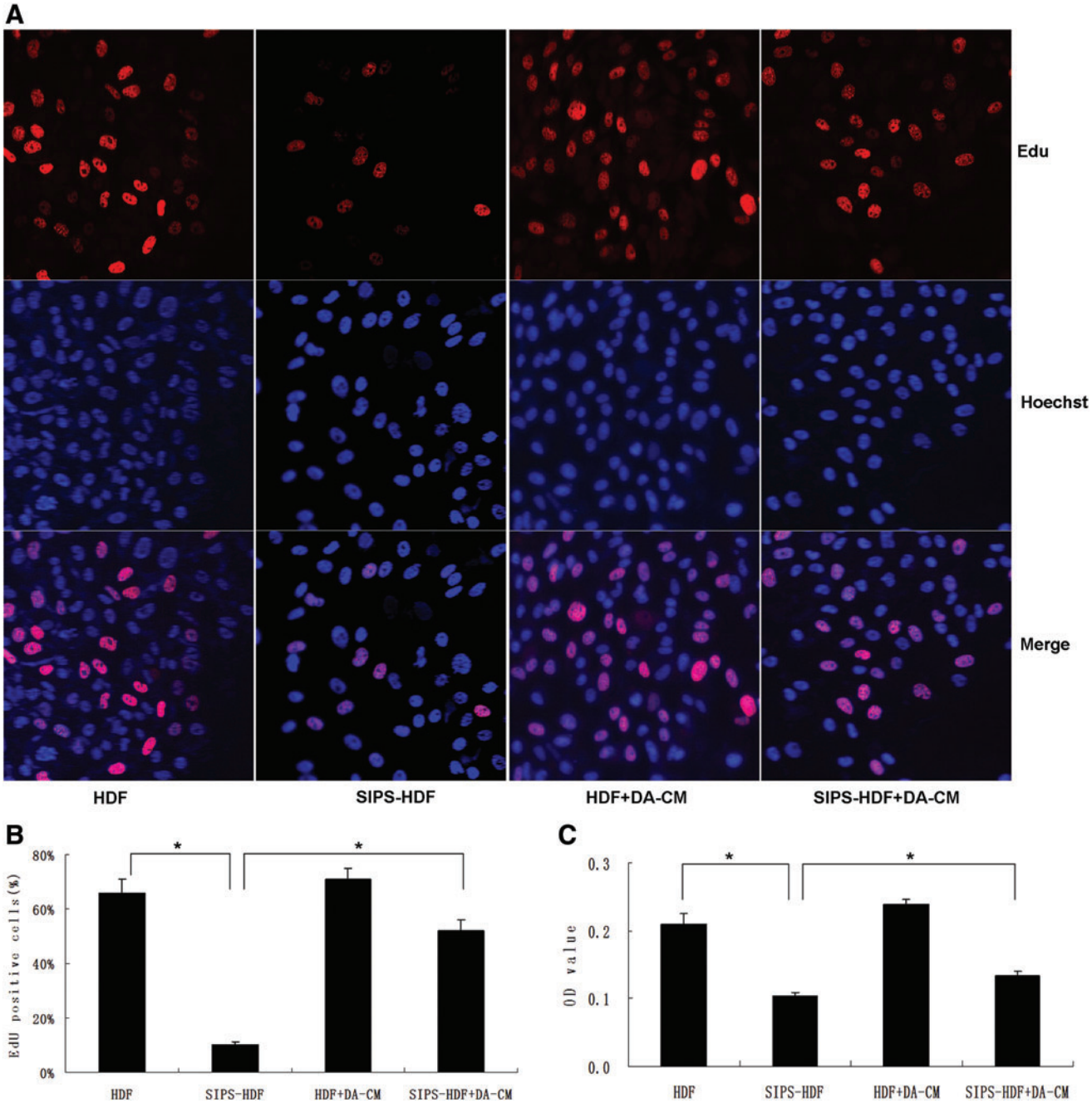

FIG. 7. DA-CM-mitigated UVB decreased cell proliferation in HDFs. HDFs were cultured in DA-CM and exposed to sham or UVB irradiation. The cells were stained by EdU and Hoechst 2 days post 5-day UVB irradiation **(A)**. The percentage of EdU-positive cells was shown **(B)**. CCK-8 assay was performed and the absorbance at 450 nm was determined using a Varioskan Flash to evaluate the proliferation ability of four groups of cells **(C)**. Data are mean ± SD, $n = 3$, $^*P < 0.05$ for SIPS-HDF versus HDF and SIPS-HDF + DA-CM versus SIPS-HDF. EdU, 5-ethynyl-2′-deoxyuridine; HDFs, human dermal fibroblasts; SIPS, stress-induced premature senescence; UVB, ultraviolet B. Color images available online at www.liebertpub.com/scd

48 h for MMP-1; 9.17 ± 0.68 vs. 5.64 ± 0.33 ng/mL at 24 h and 9.72 ± 0.57 vs. 5.96 ± 0.32 ng/mL at 48 h for MMP-3, $^*P < 0.05$). These results indicate that the reduction of collagens and induction of MMPs by UVB irradiation are largely preventable by DA-CM. The elevation of collagen production by DA-CM could be either increasing protein synthesis or reducing protein degradation by inhibition of MMPs.

TGF-β_1 in DA-CM is a major regulator in protecting the alteration of collagen types I and III, MMP-1, and MMP-3 by UVB irradiation

Having shown that DA-CM prevents alteration of collagen and MMPs by UV irradiation (Fig. 11), plus, it has been wildly accepted that TGF-β_1 is a major driving force for

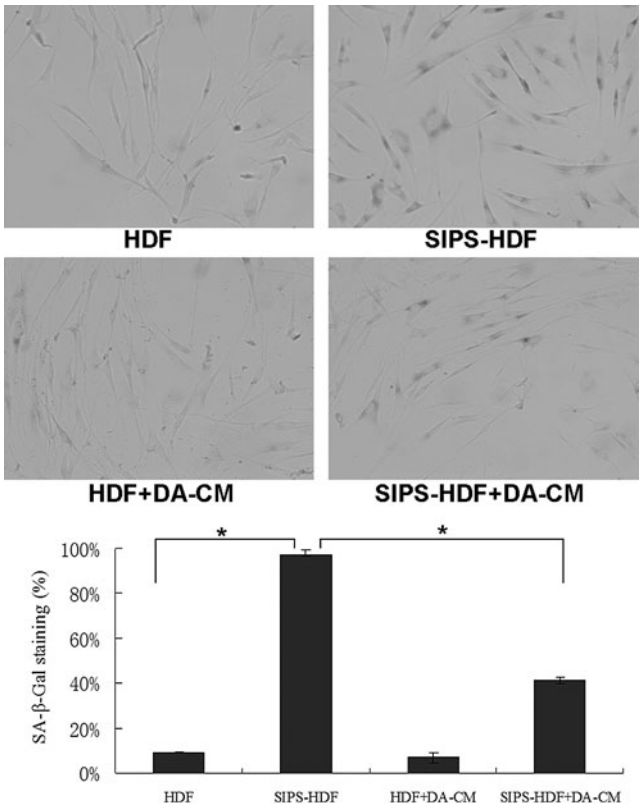

FIG. 8. DA-CM delays the premature senescence induced by repeated subcytotoxic UVB treatments in HDFs. HDFs were cultured in DA-CM and exposed to sham or subcytotoxic UV irradiation. The cellular senescence was determined by SA-β-gal staining. Premature senescence cells were positively stained. The pictures were taken under ×200 magnifications (*upper panel*). The numbers of positive stained cells were counted and statistically analyzed (*bottom panel*). Data are mean ± SD, $n = 3$, $^*P < 0.05$ for SIPS-HDF versus HDF and SIPS-HDF + DA-CM versus SIPS-HDF.

increasing collagen gene expression and reducing MMPs production. In addition, we have shown that TGF-β_1 is easily detected in DA-CM (Table 1), we next hypothesized that DA-CM prevents UV effects through secretion of TGF-β_1. To confirm this possibility, we measured protein levels

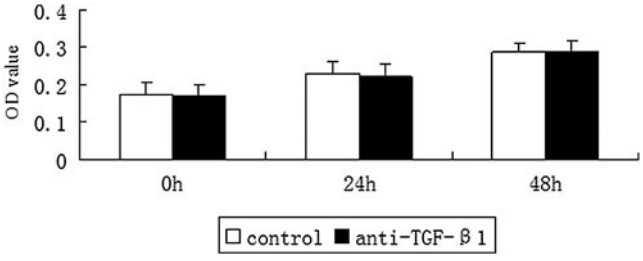

FIG. 9. TGF-β_1-neutralizing antibody does not alter HDF viability. Cultured HDFs were treated with TGF-β_1-neutralizing antibody (0.2 μg/mL). At the indicated times post treatment, the living cells were stained by the CCK-8 Kit. The cell density was determined by measuring the absorbance at 450 nm using a Varioskan Flash. Data are mean ± SD, $n = 3$. TGF-β_1, transforming growth factor-β_1.

of collagens and MMPs in a medium from UV-exposed HDFs cultured in the control medium or UV-exposed HDFs cultured in DA-CM with or without the presence of TGF-β_1-neutralizing antibody (0.2 μg/mL). The ELISA results are consistent with previous experiments; DA-CM significantly prevented UVB-induced reduction of collagen type I and type III secretion (Fig. 12A, B) and UVB-induced induction of MMP-1 and MMP-3 secretion (Fig. 12C, D). Importantly, the DA-CM effects, described above, were terminated, at least partially, by addition of TGF-β_1-neutralizing antibody (HDF + UV + DA-CM + anti-TGF-β_1 group, collagen type I: 91.07 ± 2.47 ng/mL at 24 h, 109.73 ± 1.97 ng/mL at 48 h; collagen type III: 1.31 ± 0.07 ng/mL at 24 h, 1.34 ± 0.08 ng/mL at 48 h; MMP-1: 8.45 ± 1.01 ng/mL at 24 h, 10.67 ± 0.92 ng/mL at 48 h; MMP-3: 7.80 ± 0.86 ng/mL at 24 h, 8.01 ± 0.43 ng/mL at 48 h, $^*P < 0.05$), suggesting that TGF-β_1 in the DA-CM plays an important role in protecting collagen from reduction caused by UVB in HDFs.

Discussion

It is well known that UV rays are major factors in extrinsic skin aging. UVB and ultraviolet A (UVA) rays generate severe oxidative stress in skin cells through interaction with intracellular chromophores and photosensitizers, resulting in genetic damage, replicative senescence, and connective tissue damage [20]. It is well known that the collagen in the dermis mainly comprises collagen type I (80%) and type III (10%), which are responsible for the elasticity and intensity of skin and produce a healthier skin texture [21], and decreases in both were observed in photoaging skin [22]. MMPs are a group of ECM enzymes, which can degrade all known protein components of the ECM [23]. Upregulation of MMPs caused by UV irradiation, particularly MMP-1 and MMP-3, is responsible for the lysis of dermal collagen and elastic fibers during skin aging [24–28].

SIPS refers to the accelerated aging process induced by UVB irradiation and other stimuli. Studies have proved that the repeated exposure of HDFs to UVB at subcytotoxic levels can trigger UVB-SIPS in HDFs. SIPS exhibits several biological characteristics similar to senescence, including flattened cells, positive SA-β-Gal staining, and decreased cell proliferation ability [18,29]. An in vitro photoaging mouse model can be achieved by exposure to UVB irradiation for 8 weeks [17]. The skin of photoaged mice exhibits the typical features of photoaging, such as a thickened epidermis and less disorganized collagen in the dermis. Cellular and animal models have been widely used for photoaging-related studies.

Many studies have demonstrated that DAs can be transplanted to repair damaged target tissue, similar to ADSCs. Jumabay et al. [12] demonstrated that DAs have the ability to differentiate into cardiomyocyte-like cells in vitro and in vivo. In addition, transplantation of DAs led to neovascularization in rats with myocardial infarction. Sakuma [13] also demonstrated the repair effect of DAs in the regeneration of bladder smooth muscle tissue in a mouse bladder injury model. Kim [2,30] observed high concentrations of various cytokines, such as TGF-β, bFGF, and PDGF, in the conditioned medium of ADSCs (ADSC-CM), which has been demonstrated to improve the activity of

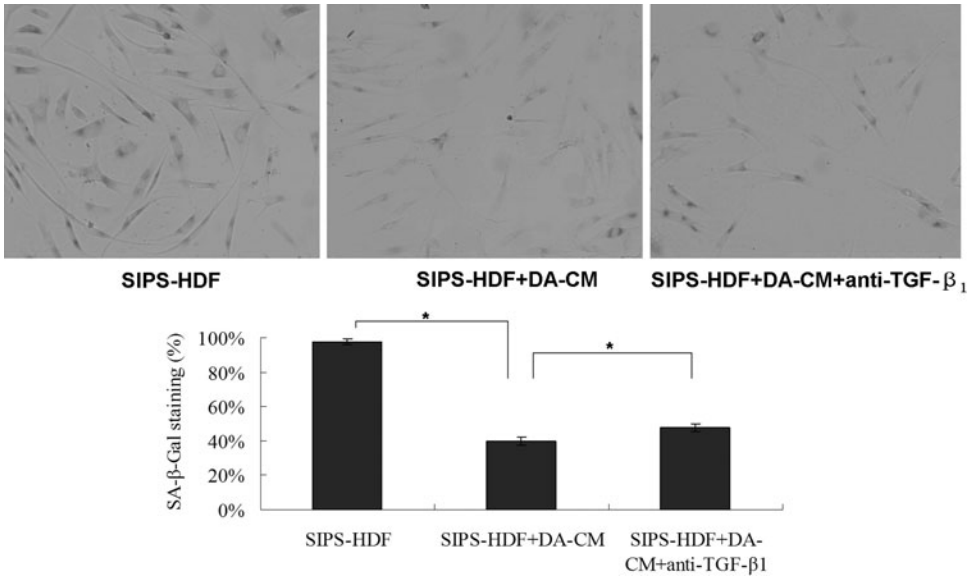

FIG. 10. TGF-β_1 in DA-CM plays a role in the anti-premature senescence process induced by repeated subcytotoxic UVB treatments in HDFs. HDFs were cultured in DA-CM and exposed to sham or subcytotoxic UV irradiation. The cellular senescence was determined by SA-β-gal staining. The pictures were taken under ×200 magnifications. Data are mean ± SD, $n = 3$, $^*P < 0.05$ for SIPS-HDF versus SIPS-HDF + DA-CM versus SIPS-HDF + DA-CM + anti-TGF-β_1.

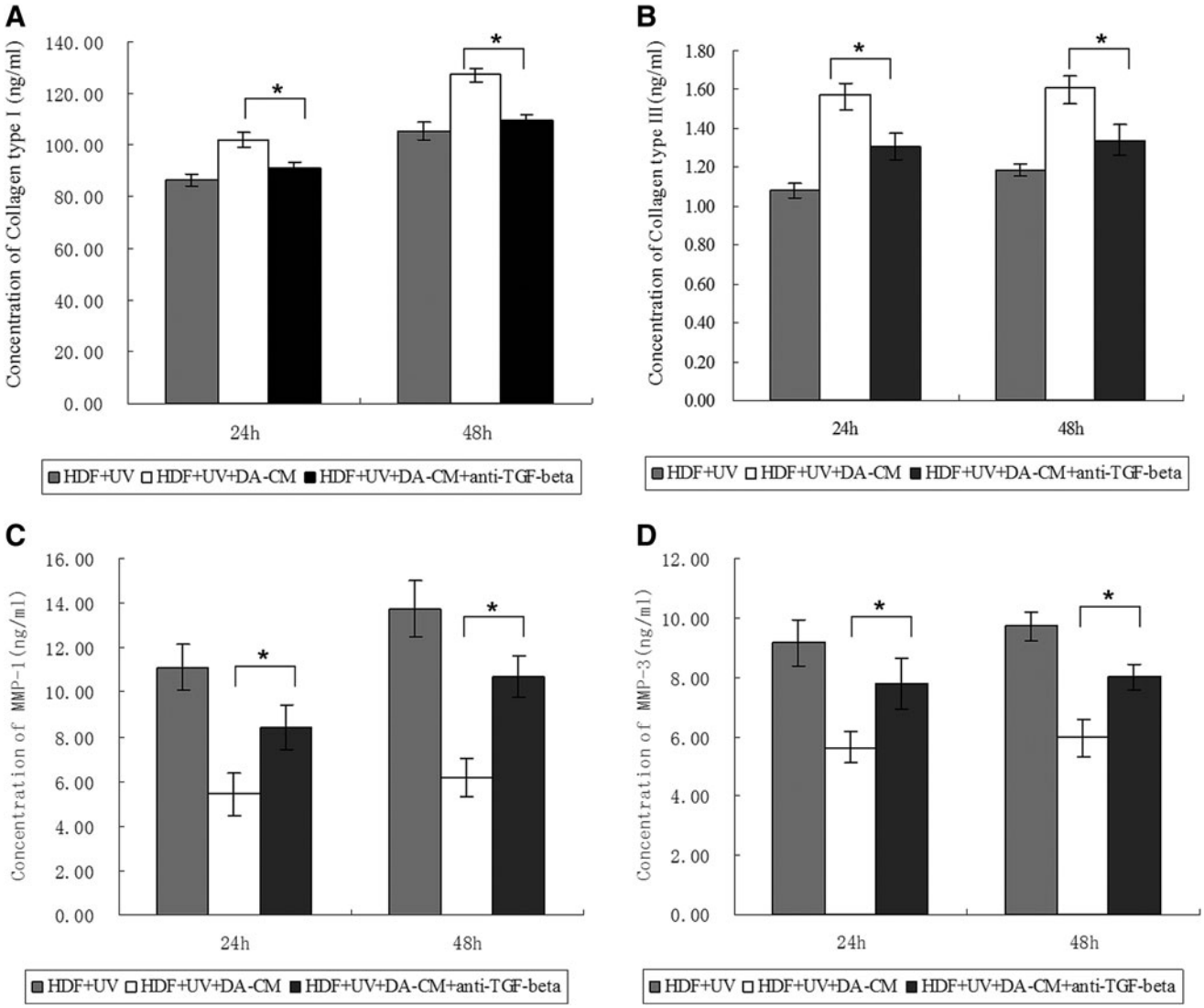

FIG. 11. DA-CM prevents UVB effects on the alteration of collagen I, collagen III, MMP-1, and MMP-3 proteins in HDFs. HDFs were cultured in DA-CM and exposed to sham or subcytotoxic UV irradiation. The medium were collected at indicated times post UV irradiation. The protein levels of collagen type I **(A)**, collagen type III **(B)**, MMP-1 **(C),** and MMP-3 **(D)** were measured by ELISA. Data are mean ± SD, $n = 3$, $^*P < 0.05$ for HDF + UV versus HDF and HDF + UV + DA-CM versus HDF + UV.

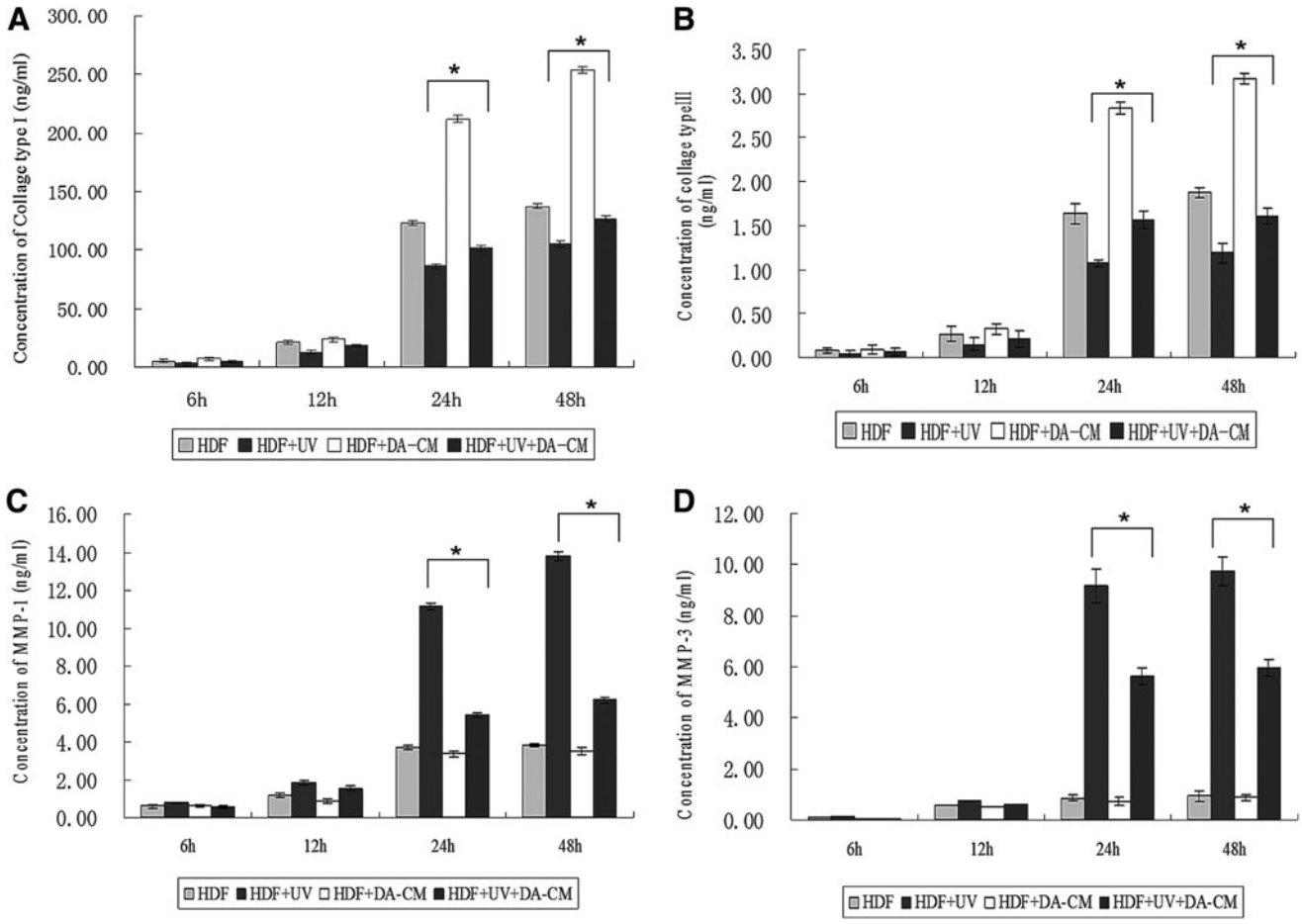

FIG. 12. TGF-β_1 in DA-CM plays a major role in preventing against the UV effects on collagen and MMPs expression. HDFs were cultured in DA-CM and treated with TGF-β_1-neutralizing antibody (0.2 μg/mL). At indicated times post sham or UVB irradiation, the cultured medium was collected and the protein levels of collagen type I **(A)**, collagen type III **(B)**, MMP-1 **(C)**, and MMP-3 **(D)** were measured by ELISA. Data are mean ± SD, $n = 3$, $^*P < 0.05$ for HDF + UV + DA-CM versus HDF + UV + DA-CM + anti-TGF-β_1.

HDFs, accelerate wound healing in animal models, and ultimately may play a major role in the antiaging process [4,31]. However, ADSCs are thought to be inhomogeneous, which limits their clinical applications and hinders in-depth research.

We have tracked PKH26-labeled Das following subcutaneous injection, and found that red fluorescence was localized only in the fat layer and not in the dermis or epidermis after 4 and 8 weeks, indicating that DAs or cells differentiated from DAs do not enter the dermis or epidermis, but only reside in adipose tissue. Furthermore, we demonstrated the influence of subcutaneously injected DAs on the dermis. Four and 8 weeks after injection, we found an increased density of more compact and orderly collagen on the injected side compared with the control side. These results prompted us to hypothesize that some secretory factors from DAs might influence the content and density of collagens in the dermis, although DAs reside in the adipose tissue.

We further validated the effect of DA exocrine factors on the skin of photoaged mice. Histopathology showed that collagen density showed an obvious increase in the DA-CM-injected side compared with the control, with H&E and Masson trichrome staining. Upon immunohistochemical staining for collagens and MMPs, the percentages of stained areas of types I and III collagen were significantly higher, whereas those of MMP-1 and MMP-3 were not, compared with the control, indicating the increased expression of types I and III collagen on the treated side. The epidermis showed no obvious change between the injected and control sides. This could be because the secreted factors might be consumed in the dermis and could not directly influence the epidermis.

Several cytokines, including HGF, FGF-1, G-CSF, GM-CSF, IL-6, VEGF, and TGF-β, have been detected in ADSC-CM, and TGF-β has an important role [32,33]. Poloni et al. [34] demonstrated that DAs showed properties similar to those of ADSCs, including the types of cytokines secreted. These cytokines play important roles in the repair process of DAs and ADSCs. Ohta [35] proved that some neurotrophic factors, such as brain-derived neurotrophic factor (BDNF) and glial cell line-derived neurotrophic factor (GDNF), derived from grafted DAs mainly contribute to the promotion of functional recovery from SCI-induced motor dysfunction in rats.

In our study, we found different concentrations of cytokines in DA-CM, including PDGF, bFGF, VEGF, KGF,

TGF-β_1, and HGF, which may attribute to the antiphotoaging process. Previous literature has confirmed that these cytokines are enrolled in the process of stimulating the proliferation and activity of fibroblasts and promoting the synthesis of the ECM. Researchers have demonstrated the modulation effect of TGF-β, especially TGF-β_1, in collagen synthesis and degradation during skin photoaging [34,35].TGF-β_1 induces the migration and proliferation of fibroblasts, contributes to increased collagen synthesis [36], and triggers the downregulation of MMP-1, thereby sustaining the subtle balance between collagen synthesis and degradation [37,38]. UV and other stimuli can damage the TGF-β pathway, which in turn causes a reduction in collagen synthesis and an increase in the degradation activity of MMPs, resulting in skin aging [39,40]. Therefore, we proposed that TGF-β_1 and other cytokines in the conditioned medium of DA might intervene in collagen synthesis and degradation processes and furthermore protect HDFs from UV-induced damage.

To prove this, we used concentrated DA-CM to culture UVB-SIPS HDFs, and the results were in agreement with this hypothesis. DA-CM not only protected HDFs from UVB-induced decreased cell proliferation and premature senescence but also increased the content of collagen. We found that SIPS-HDFs were less proliferated and in apparent premature aging, presenting an enlarged flattened cell morphology and more positive SA-β-Gal staining. However, in the SIPS-HDF + DA-CM group, higher percentage of EdU staining cells and more fusiform HDFs with less positive SA-β-Gal staining were found. These indicated that the secreted factors in DA-CM could significantly mitigate the decreased cell proliferation and delay premature senescence in HDFs induced by UVB, showing a potential antiphotoaging effect. And the neutralization of TGF-β_1 partially decreased the protection effect, indicating the effect of TGF-β_1 in this process. After one dosage of 30 mJ/cm^2 UVB irradiation, DA-CM-treated groups showed higher collagen types I and III contents and lower MMP-1 and MMP-3 contents than their counterparts after 24 h. We also used neutralizing antibodies to hinder the function of TGF-β_1 and found that the repair effect of DA-CM on UV-damaged HDFs can be mainly attributed to TGF-β_1 in terms of increased collagen synthesis and decreased MMP-1 and MMP-3. Taken together, DA-CM, especially TGF-β_1, can alleviate the photoaging process by delaying UVB-induced premature senescence and regulating collagen synthesis and degradation. Additionally, other factors also are important in this process; these are worthy of further investigation.

Many factors impairing DNA, including UVB irradiation, can trigger phosphorylation of histone H2AX on Ser-139 [41,42]. We further confirmed the effect of TGF-β_1 on DNA damage caused by UVB in HDFs. In Supplementary Fig. S3, two groups of HDFs, one group with added 3 ng/mL TGF-β_1, were irradiated by single dosage of 30 mJ/cm^2 UVB. After 0, 8, and 24 h, the percentages of positive-stained cells of γH2AX were not significantly different from the control group, indicating that TGF-β_1 cannot protect HDFs from UVB-induced DNA damage. The antiphotoaging effect of TGF-β_1 may mainly lies in the regulation of collagen synthesis and degradation, while not in protection from DNA damage. It is consistent with the former findings by Quan [43] that TGF-β is a critical regulator of type I procollagen synthesis, and UV-induced impair in the TGF-β/Smad pathway is a critical molecular mechanism in the pathophysiology of photoaging.

Our experiments on photoaging mice revealed significant changes in collagen staining, but not in MMP-1 and MMP-3 in DA-CM-injected skin compared with the control, which might be caused by the relatively lower amounts of MMP-1 and 3 in the dermis or the relative long time between the last treatment and skin biopsies on the 4th and 8th weeks. We also reviewed previous related studies and found most of those were about changes on MMPs less than 5 days after intervention [44–46], lacking long-term observation reports. On the other hand, in the cell-based experiments, changes in the concentration of MMPs could be accurately detected by ELISA, and we conducted an ELISA experiment within 48 h; therefore, we were able to observe changes between the treated and untreated groups.

There have been no previous reports regarding the antiphotoaging effect of DAs in vivo and in vitro. This is the first study to suggest that DAs could be a promising tool for the repair of photoaging and that the underlying mechanism involves cytokines in the conditioned medium secreted by DAs, especially TGF-β_1, which hinders the premature senescence and causes the increased synthesis and decreased degradation of collagen. Because adipose tissue is abundant and easily accessible at most ages in humans, DAs and cytokines secreted by DAs may be an attractive therapeutic strategy for photoaged skin.

Acknowledgments

This project is supported by grants from the Chinese National Natural Science Foundation (81301384 and 81000700), Jiangsu Province Natural Science Foundation (BK20131029 and BK2012877), and Jiangsu Province Research and Innovation Program for Graduates (2012).

Author Disclosure Statement

All authors declare that they have no conflicts of interest.

References

1. Berneburg M, H Plettenberg and J Krutmann. (2000). Photoaging of human skin. Photodermatol Photoimmunol Photomed 16:239–244.
2. Kim WS, BS Park and JH Sung. (2009). Protective role of adipose-derived stem cells and their soluble factors in photoaging. Arch Dermatol Res 301:329–336.
3. Kim WS, BS Park, SH Park, HK Kim and JH Sung. (2009). Antiwrinkle effect of adipose-derived stem cell: activation of dermal fibroblast by secretory factors. J Dermatol Sci 53:96–102.
4. Kim WS, BS Park, JH Sung, JM Yang, SB Park, SJ Kwak and JS Park. (2007). Wound healing effect of adipose-derived stem cells: a critical role of secretory factors on human dermal fibroblasts. J Dermatol Sci 48:15–24.
5. Kim H, K Choi, OK Kweon and WH Kim. (2012). Enhanced wound healing effect of canine adipose-derived mesenchymal stem cells with low-level laser therapy in athymic mice. J Dermatol Sci 68:149–156.
6. Zuk PA, M Zhu, P Ashjian, DA De Ugarte, JI Huang, H Mizuno, ZC Alfonso, JK Fraser, P Benhaim and MH

Hedrick. (2002). Human adipose tissue is a source of multipotent stem cells. Mol Biol Cell 13:4279–4295.
7. Halvorsen YD, D Franklin, AL Bond, DC Hitt, C Auchter, AL Boskey, EP Paschalis, WO Wilkison and JM Gimble. (2001). Extracellular matrix mineralization and osteoblast gene expression by human adipose tissue-derived stromal cells. Tissue Eng 7:729–741.
8. Tholpady SS, R Llull, RC Ogle, JP Rubin, JW Futrell and AJ Katz. (2006). Adipose tissue: stem cells and beyond. Clin Plast Surg 33:55–62, vi.
9. Yagi K, D Kondo, Y Okazaki and K Kano. (2004). A novel preadipocyte cell line established from mouse adult mature adipocytes. Biochem Biophys Res Commun 321: 967–974.
10. Matsumoto T, K Kano, D Kondo, N Fukuda, Y Iribe, N Tanaka, Y Matsubara, T Sakuma, A Satomi, et al. (2008). Mature adipocyte-derived dedifferentiated fat cells exhibit multilineage potential. J Cell Physiol 215:210–222.
11. Kikuta S, N Tanaka, T Kazama, M Kazama, K Kano, J Ryu, Y Tokuhashi and T Matsumoto. (2013). Osteogenic effects of dedifferentiated fat cell transplantation in rabbit models of bone defect and ovariectomy-induced osteoporosis. Tissue Eng Part A 19:1792–1802.
12. Jumabay M, T Matsumoto, S Yokoyama, K Kano, Y Kusumi, T Masuko, M Mitsumata, S Saito, A Hirayama, H Mugishima and N Fukuda. (2009). Dedifferentiated fat cells convert to cardiomyocyte phenotype and repair infarcted cardiac tissue in rats. J Mol Cell Cardiol 47:565–575.
13. Sakuma T, T Matsumoto, K Kano, N Fukuda, D Obinata, K Yamaguchi, T Yoshida, S Takahashi and H Mugishima. (2009). Mature, adipocyte derived, dedifferentiated fat cells can differentiate into smooth muscle-like cells and contribute to bladder tissue regeneration. J Urol 182:355–365.
14. Sugihara H, N Yonemitsu, S Miyabara and K Yun. (1986). Primary cultures of unilocular fat cells: characteristics of growth in vitro and changes in differentiation properties. Differentiation 31:42–49.
15. Wang Y, L Zhao and BM Hantash. (2010). Support of human adipose-derived mesenchymal stem cell multipotency by a poloxamer-octapeptide hybrid hydrogel. Biomaterials 31:5122–5130.
16. Huang J, S Wang, C Wei, Y Xu, Y Wang, J Jin and G Teng. (2011). In vivo differentiation of adipose-derived stem cells in an injectable poloxamer-octapeptide hybrid hydrogel. Tissue Cell 43:344–349.
17. Takeuchi H, T Gomi, M Shishido, H Watanabe and N Suenobu. (2010). Neutrophil elastase contributes to extracellular matrix damage induced by chronic low-dose UV irradiation in a hairless mouse photoaging model. J Dermatol Sci 60:151–158.
18. Debacq-Chainiaux F, C Borlon, T Pascal, V Royer, F Eliaers, N Ninane, G Carrard, B Friguet, F de Longueville, et al. (2005). Repeated exposure of human skin fibroblasts to UVB at subcytotoxic level triggers premature senescence through the TGF-beta1 signaling pathway. J Cell Sci 118:743–758.
19. Zhou BR, XF Guo, JA Zhang, Y Xu, W Li, D Wu, ZQ Yin, F Permatasari and D Luo. (2013). Elevated miR-34c-5p mediates dermal fibroblast senescence by ultraviolet irradiation. Int J Biol Sci 9:743–752.
20. Ma W, M Wlaschek, I Tantcheva-Poor, LA Schneider, L Naderi, Z Razi-Wolf, J Schuller and K Scharffetter-Kochanek. (2001). Chronological ageing and photoageing of the fibroblasts and the dermal connective tissue. Clin Exp Dermatol 26:592–599.
21. Gelse K, E Poschl and T Aigner. (2003). Collagens—structure, function, and biosynthesis. Adv Drug Deliv Rev 55:1531–1546.
22. Talwar HS, CE Griffiths, GJ Fisher, TA Hamilton and JJ Voorhees. (1995). Reduced type I and type III procollagens in photodamaged adult human skin. J Invest Dermatol 105:285–290.
23. Bramono DS, JC Richmond, PP Weitzel, DL Kaplan and GH Altman. (2004). Matrix metalloproteinases and their clinical applications in orthopaedics. Clin Orthop Relat Res:272–285.
24. Fisher GJ, SC Datta, HS Talwar, ZQ Wang, J Varani, S Kang and JJ Voorhees. (1996). Molecular basis of sun-induced premature skin ageing and retinoid antagonism. Nature 379:335–339.
25. Rabe JH, AJ Mamelak, PJ McElgunn, WL Morison and DN Sauder. (2006). Photoaging: mechanisms and repair. J Am Acad Dermatol 55:1–19.
26. Hornebeck W. (2003). Down-regulation of tissue inhibitor of matrix metalloprotease-1 (TIMP-1) in aged human skin contributes to matrix degradation and impaired cell growth and survival. Pathol Biol (Paris) 51:569–573.
27. Quan T, Z Qin, W Xia, Y Shao, JJ Voorhees and GJ Fisher. (2009). Matrix-degrading metalloproteinases in photoaging. J Investig Dermatol Symp Proc 14:20–24.
28. Li Y, W Xia, Y Liu, HA Remmer, J Voorhees and GJ Fisher. (2013). Solar ultraviolet irradiation induces decorin degradation in human skin likely via neutrophil elastase. PLoS One 8:e72563.
29. Chen W, J Kang, J Xia, Y Li, B Yang, B Chen, W Sun, X Song, W Xiang, et al. (2008). p53-related apoptosis resistance and tumor suppression activity in UVB-induced premature senescent human skin fibroblasts. Int J Mol Med 21:645–653.
30. Kim WS, BS Park and JH Sung. (2009). The wound-healing and antioxidant effects of adipose-derived stem cells. Expert Opin Biol Ther 9:879–887.
31. Kim JH, M Jung, HS Kim, YM Kim and EH Choi. (2011). Adipose-derived stem cells as a new therapeutic modality for ageing skin. Exp Dermatol 20:383–387.
32. Moon KM, YH Park, JS Lee, YB Chae, MM Kim, DS Kim, BW Kim, SW Nam and JH Lee. (2012). The effect of secretory factors of adipose-derived stem cells on human keratinocytes. Int J Mol Sci 13:1239–1257.
33. Kim WS, SH Park, SJ Ahn, HK Kim, JS Park, GY Lee, KJ Kim, KK Whang, SH Kang, BS Park and JH Sung. (2008). Whitening effect of adipose-derived stem cells: a critical role of TGF-beta 1. Biol Pharm Bull 31:606–610.
34. Poloni A, G Maurizi, P Leoni, F Serrani, S Mancini, A Frontini, MC Zingaretti, W Siquini, R Sarzani and S Cinti. (2012). Human dedifferentiated adipocytes show similar properties to bone marrow-derived mesenchymal stem cells. Stem Cells 30:965–974.
35. Ohta Y, M Takenaga, Y Tokura, A Hamaguchi, T Matsumoto, K Kano, H Mugishima, H Okano and R Igarashi. (2008). Mature adipocyte-derived cells, dedifferentiated fat cells (DFAT), promoted functional recovery from spinal cord injury-induced motor dysfunction in rats. Cell Transplant 17:877–886.
36. Desmouliere A, A Geinoz, F Gabbiani and G Gabbiani. (1993). Transforming growth factor-beta 1 induces alpha-smooth muscle actin expression in granulation tissue

myofibroblasts and in quiescent and growing cultured fibroblasts. J Cell Biol 122:103–111.
37. Yuan W and J Varga. (2001). Transforming growth factor-beta repression of matrix metalloproteinase-1 in dermal fibroblasts involves Smad3. J Biol Chem 276:38502–38510.
38. Philipp K, F Riedel, G Germann, K Hormann and M Sauerbier. (2005). TGF-beta antisense oligonucleotides reduce mRNA expression of matrix metalloproteinases in cultured wound-healing-related cells. Int J Mol Med 15:299–303.
39. Baker DJ, T Wijshake, T Tchkonia, NK LeBrasseur, BG Childs, B van de Sluis, JL Kirkland and JM van Deursen. (2011). Clearance of p16Ink4a-positive senescent cells delays ageing-associated disorders. Nature 479:232–236.
40. Ludwig S, A Klitzsch and A Baniahmad. (2012). The ING tumor suppressors in cellular senescence and chromatin. Cell Biosci 1:25.
41. Sedelnikova OA, DR Pilch, C Redon and WM Bonner. (2003). Histone H2AX in DNA damage and repair. Cancer Biol Ther 2:233–235.
42. Halicka HD, X Huang, F Traganos, MA King, W Dai and Z Darzynkiewicz. (2005). Histone H2AX phosphorylation after cell irradiation with UV-B: relationship to cell cycle phase and induction of apoptosis. Cell Cycle 4:339–345.
43. Quan T, T He, S Kang, JJ Voorhees and GJ Fisher. (2002). Ultraviolet irradiation alters transforming growth factor beta/smad pathway in human skin in vivo. J Invest Dermatol 119:499–506.
44. Eto H, H Suga, N Aoi, H Kato, K Doi, S Kuno, Y Tabata and K Yoshimura. (2012). Therapeutic potential of fibroblast growth factor-2 for hypertrophic scars: upregulation of MMP-1 and HGF expression. Lab Invest 92:214–223.
45. Park M, J Han, CS Lee, BH Soo, KM Lim and H Ha. (2013). Carnosic acid, a phenolic diterpene from rosemary, prevents UV-induced expression of matrix metalloproteinases in human skin fibroblasts and keratinocytes. Exp Dermatol 22:336–341.
46. Song KC, TS Chang, H Lee, J Kim, JH Park and GS Hwang. (2012). Processed panax ginseng, sun ginseng increases type I collagen by regulating MMP-1 and TIMP-1 expression in human dermal fibroblasts. J Ginseng Res 36:61–67.

Address correspondence to:
Prof. Dan Luo
Department of Dermatology
The First Affiliated Hospital of Nanjing Medical University
Nanjing 210029
China

E-mail: daniluo2005@163.com

Dr. Bing-rong Zhou
Department of Dermatology
The First Affiliated Hospital of Nanjing Medical University
Nanjing 210029
China

E-mail: bingrong.2002@163.com

Received for publication July 8, 2014
Accepted after revision December 3, 2014
Prepublished on Liebert Instant Online December 17, 2014